IEEE Access
Multidisciplinary | Rapid Review | Open Access Journal

Received February 12, 2020, accepted February 19, 2020, date of publication February 21, 2020, date of current version March 2, 2020.

Digital Object Identifier 10.1109/ACCESS.2020.2975562

Adaptive Noise Reduction Method of Synchronous Hydraulic Motor Acoustic Signal Based on Improved Dislocation Superposition Method

NING DAYONG[1], SUN HONGYU[1], XU AOYU[1], GONG YONGJUN[1], DU HONGWEI[1], AND HOU JIAOYI[1,2]

[1]National Center for International Research of Subsea Engineering Technology and Equipment, Dalian Maritime University, Dalian 116026, China
[2]State Key Laboratory of Fluid Power and Mechatronic Systems, Dalian Maritime University, Dalian 116026, China

Corresponding author: Hou Jiaoyi (houjiaoyi@163.com)

This work was supported in part by the National Key Research and Development Program under Grant 2018YFC0810404 and Grant 2018YFC0810406, in part by the Fundamental Research Funds for the Central Universities under Grant 3132019118, and in part by the Open Foundation of the State Key Laboratory of Fluid Power and Mechatronic Systems under Grant GZKF-201810.

ABSTRACT Acoustic signal contains information on the state of mechanical motion, but the disadvantage of low signal-to-noise ratio (SNR) is that acoustic signal without noise reduction is difficult to apply to fault diagnosis directly. This study proposes an adaptive noise reduction method based on the dislocation superposition method (DSM), which can realize automatic noise reduction for acoustic signals of low SNR synchronous hydraulic motors. First, the theoretical rotation period of the synchronous hydraulic motor is obtained according to the flow meter. Then, the actual signal is subjected to DSM processing according to the measurement accuracy of the flow meter and the theoretical rotation period to adjust the exact superposition length and the initial position of the actual signal. Finally, when the stop condition is not satisfied, the number of superposition is increased and the above process is repeated. The superimposed signal satisfying the stop condition is taken as the noise reduction signal. According to experimental results, the proposed method has good noise reduction effect on the acoustic signals of the synchronous hydraulic motor health state, wear out state of gear and end cover, and rust state of the gear. The noise reduction signal has been verified to have higher accuracy than the actual signal. Therefore, the proposed automatic noise reduction method can be applied to the noise reduction processing of other kinds of rotating mechanical acoustic signals.

INDEX TERMS Dislocation superposition method (DSM), acoustic signal, adaptive method, automatic noise reduction, synchronous hydraulic motor.

I. INTRODUCTION

Synchronous hydraulic motors are common mechanical components in high-load hydraulic synchronous operations. Failure of motor operations can cause severe economic losses or even personal accidents. At present, synchronous hydraulic motor fault detection mainly determines a fault by observing the system pressure and the motion state of the actuator. Existing methods for evaluating the state of mechanical equipment often use non-destructive testing methods such as acoustic, vibration, and acoustic emission signals. During the acquisition process of the vibration signal, the sensor needs to be in close contact with the surface of the workpiece to be tested, and the installation process is cumbersome. The acoustic emission sensor needs to be kept close to the device to be tested. The advantage of using an acoustic signal is that the acoustic signal is easy to acquire, the detection process is simple, and the cost of the ordinary acoustic sensor is low [1], [2]. The mechanical equipment acoustic signal has three categories of components, namely, the acoustic signal of the component to be analyzed, other components, and background noise. The acoustic signal of the component to be analyzed is usually referred to as a valid signal, and the other two are collectively referred to as noise [3].

The associate editor coordinating the review of this manuscript and approving it for publication was Lorenzo Mucchi.

Owing to the combined effects of acoustic signals and background noise from other components, valid signals are often severely obscured by various noises. Therefore, if noise is not adequately reduced, then reliable condition monitoring cannot be performed [4].

The traditional signal denoising method uses a Fourier transform-based filter to filter the frequency components of noise but has apparent defects in the case of non-stationary signals and short-term transient signals. Currently, popular methods of noise reduction include wavelet transform (WT) [5], empirical mode decomposition (EMD) [6], Savitzky-Golay (S-G) filter [7], dislocation superposition method (DSM) [8] et al.

WT is a widely used signal processing tool. The tool can provide signal information in time and frequency domains, as well as indicate but also has multi-scale characteristics. Thus, WT can decompose signal into multiple components with different components and then reconstruct denoised signal with a single component [9]. Parey and Singh [10] used continuous WT to denoise the angle domain signal of gearbox acoustic signal. Wang and He [11] used wavelet packet manifold to suppress effectively the noise of rolling bearing. Chegini *et al.* [12] used empirical WT to reduce the noise of bearing vibration signal. Chen *et al.* [13] used the wavelet soft threshold method to denoise the low-frequency oscillating signal of the power system, and the effect is good. On the basis of wavelet noise reduction, many scholars have proposed better performance noise reduction methods. Wang and Lee [14] combined spectral subtraction method and empirical wavelet transform to denoising signals and extract the gear faults' side-band feature, the proposed method has better processing effect than traditional wavelet noise reduction. Qin *et al.* [15], [16] proposed dense framelets with two generators and M-band flexible WT. The dense framelets with two generators have better denoising performance and shift-invariance than orthogonal wavelets and had higher density framelets. The M-band flexible wavelet transform has better denoising performance than flexible, orthogonal, and biorthogonal wavelets. Although many studies focused on wavelet noise reduction, different wavelet bases have different effects on signal analysis, and there is still no clear standard has been established on how to choose a suitable wavelet base for different signals [17].

EMD can decompose the AM–FM signal into the sum of intrinsic mode function (IMF), which has distinct advantages in processing non-stationary and non-linear data. Therefore, EMD is used in signal noise reduction. Li *et al.* [18] used the simplified EMD algorithm to extract features from the hydrophone signals of a centrifugal pump with strong background noise, which can effectively suppress noise and obtain precise pulses. To improve the noise reduction effect of EMD, many scholars have proposed improved methods based on EMD. Zhang *et al.* [19] proposed a signal denoising method named EMD-AdaptiveP, it combined similar strategy of wavelet filtering and EMD and had better noise reduction performance than traditional EMD method. Li *et al.* [20], [21] proposed complete ensemble empirical mode decomposition with adaptive noise on the basis of EMD and uniform phase empirical mode decomposition to implement noise reduction processing on underwater acoustic signals and achieved good results. Although studies have been done on noise reduction using many EMD-based methods, it has problems such as modal mixing and poor processing effect on low signal-to-noise ratio signals [22], [23]. Therefore, compared to signal noise reduction, EMD is used more often to extract signal features, and its actual effect on signal noise reduction is not as good as WT.

Scholars have proposed some other methods for signal noise reduction processing. Chen *et al.* [7] proposed a signal denoising method based on S-G filter in low-frequency oscillation signals. But when the SNR is low, the noise reduction effect of the S-G method is not good enough. Ning *et al.* [8] proposed the DSM in 2015. Compared with other methods, DSM only has time-domain calculation. By periodic superposition of the actual signal, the signal-to-noise ratio of the practical component can be improved without destroying the practical component. This method avoids the modal mixing problem of many noise reduction methods, it can retain specific frequency details, and abnormal mutation information related to the fault frequency can also be retained. However, under the condition of non-stationary and quasi-periodic signals, determining the starting point of each signal cycle manually is necessary. Ning *et al.* [3] used the improved DSM to extract automatically the fault components of engine quasi-periodic acoustic signals with excellent results. However, this method needs to use the pulse data of the encoder to find the starting position of each signal cycle accurately. Thus, the synchronous hydraulic motor cannot install the encoder. Consequently, this method cannot be applied.

This study proposes an adaptive noise reduction method for acoustic signals of synchronous hydraulic motors based on improved DSM. The essence of the method is to superimpose the actual signal in the time domain, avoiding the shortcoming of modal confusion, and processing the low signal ratio acoustic signal well. The proposed method can adaptively select the starting point, length, and number of superpositions. The degree of noise reduction can be changed by adjusting the parameters within the algorithm, and the process of noise reduction processing of synchronous hydraulic motor acoustic signals can be automated.

II. DSM REVIEW

To make the proposed method easier to understand, first review the traditional DSM. According to [8], the mathematical expression of DSM is as follows:

$$\tilde{x}(n) = \frac{1}{K+1} \sum_{k=0}^{K} x(n + kL), \tag{1}$$

where $x(n)$ is the actual signal, $\tilde{x}(n)$ is the signal processed by DSM (named superimposed signal), K represents the number of superpositions ($K = 0, 1, 2 \ldots$), and L is the superimposed

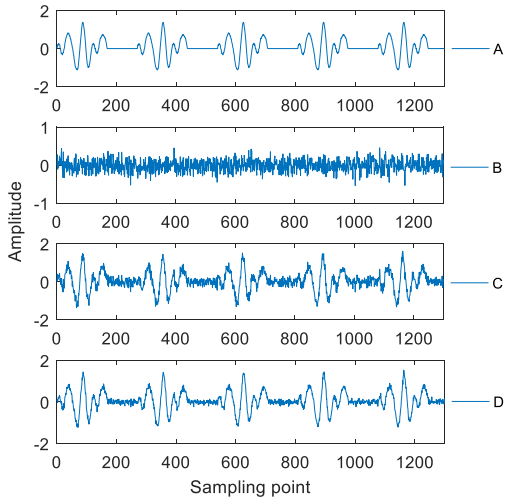

FIGURE 1. Schematic of dislocation superposition method (DSM). A is the effective component of the signal; B is the interference signal; C is the mixed signal of A and B; D is the superimposed signal obtained when the number of superpositions is 5. After DSM processing, the signal-to-noise ratio of the superimposed signal D becomes higher than signal C.

length (period of the signal to be processed). FIGURE 1 is a graphical illustration of DSM processing results.

A is the target signal, B is the interference signal, C is the mixed signal of A and B, and signal D is the superposition signal obtained from signal C by using equation (1). The number of superimpositions is $K = 5$, and the superposition length L is the period of signal A. Compared with signal C, the component proportion of the target signal in signal D is larger, and the proportion of the interference signal is smaller. To facilitate understanding, the kth superimposed signal in the superimposed signal $\tilde{x}(n)$ is referred to as the superposition component, and is denoted as SC_k.

$$SC_k = x(n + kL) \tag{2}$$

Pearson's correlation coefficient is used to compare the similarity between the target and the superimposed signals to test the DSM processing effect [24]. The expressions of Pearson's correlation coefficient for A and D are as follows:

$$\begin{aligned}\rho_{A(n),D(n)} &= \frac{\langle A(n), D(n)\rangle}{\sqrt{\langle A(n), A(n)\rangle}\sqrt{\langle D(n), D(n)\rangle}} \\ &= \frac{\sum_{i=1}^{N}[A(i) \times D(i)]}{\sqrt{\sum_{i=1}^{N}[A(i) \times A(i)]}\sqrt{\sum_{i=1}^{N}[D(i) \times D(i)]}}\end{aligned} \tag{3}$$

where N is the sampling points of A and D, and $<.>$ is the inner product. According to the Cauchy–Schwarz inequality, the scope of $\rho_{A(n),E(n)}$ is:

$$-1 \leq \rho_{A(n),E(n)} \leq 1. \tag{4}$$

The closer the Pearson's correlation coefficient is to 0, the weaker the linear correlation between the two signals. When the correlation coefficient is equal to 1, the two signals are identical. The judgment of the correlation coefficient size depends on the specific use of background and purpose [25].

In theory, the DSM algorithm can extract the periodic target signal from the mixed signal with low SNR. The accuracy of the extraction result increases with the increase in the number of superpositions.

In actual signal processing, superimposed length is constant, and therefore causes multiple superimposed end effector. To extract features accurately, a window function can be used to extract the middle part of the superimposed signal for subsequent processing. Examples of end effects and window functions are shown in FIGURE 2.

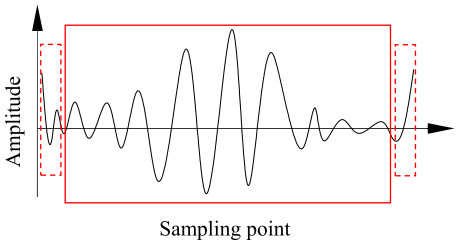

FIGURE 2. Example of superimposed signal end effect and pre-processing before signal feature extraction. The inside of the dotted rectangular frame is the end effect signal with abnormal frequency components. The solid rectangular frame is an artificially defined window function, which is used to retain the accurate signal frequency components.

III. INTRODUCTION OF ADAPTIVE NOISE REDUCTION METHOD BASED ON IMPROVED DSM

To realize the automatic noise reduction of the acoustic signal of the synchronous hydraulic motor, an automatic noise reduction method based on DSM is proposed, and the proposed method will be described below.

A. FACTORS AFFECTING DSM TREATMENT EFFECT

Owing to various errors in the system, the existence of the gear-type synchronous hydraulic motor changes, such that the synchronous hydraulic motor acoustic signal belongs to the quasi-periodic signal. FIGURE 3 shows a quasi-periodic signal sample.

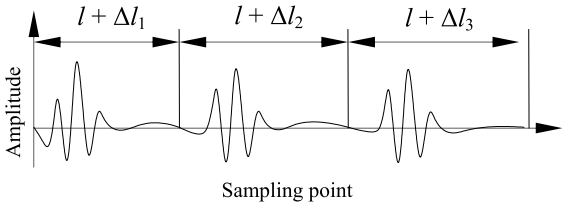

FIGURE 3. Quasi-periodic signal diagram. l is the average length of the quasi-periodic signal, and Δl_1, Δl_2, and Δl_3 represent the deviation values of the length of each period, respectively.

When the superimposed length is different from the average period of the quasi-periodic signal, a phase difference is observed in the effective information in the *SC*s when the number of superpositions is different, and the effective information will be destroyed after the superposition processing, as shown in FIGURE 4.

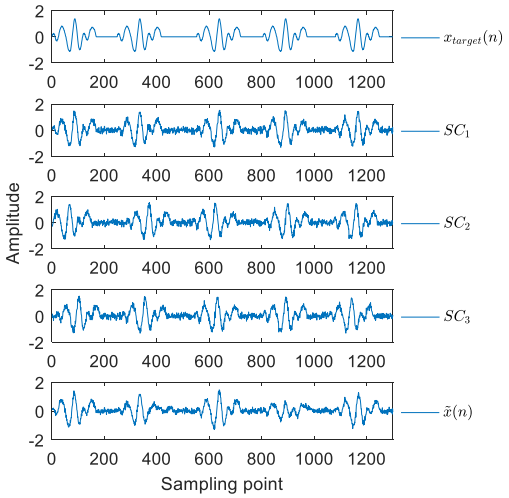

FIGURE 4. Schematic diagram of the DSM processing effect when the superposition length is different from the actual signal average period length. $x_{target}(n)$ represents the target signal. SC_1, SC_2, SC_3 are three consecutive superimposed components in $x_{target}(n)$ containing noise. $\tilde{x}(n)$ is the superimposed signal, where $\tilde{x}(n) = (SC_1 + SC_2 + SC_3)/3$. The effective signal component of the signal in $\tilde{x}(n)$ is remarkably different from $x_{target}(n)$, and the noise reduction effect is not ideal.

The superimposed length of the traditional DSM algorithm cannot be automatically adjusted. When the signal is quasi-periodic, the starting point and the superimposed length of each *SC* needs to be manually selected. Ning *et al.* [3] used the improved DSM to extract automatically the fault components of an engine's quasi-periodic acoustic signal. However, this method utilizes the encoder to position accurately the relative position of the acoustic signal with the rotation period, and the synchronous hydraulic motor cannot install the encoder. Therefore, the method cannot be used.

The proposed method calculates the theoretical period of the acoustic signal of the synchronous hydraulic motor through the flow meter and fixed parameters. The optimal stack length based on the theoretical period length is determined, and the impact of the metering accuracy of the flow meter itself on the actual cycle is reduced. When the position of the starting point of the actual signal changes, the relative position of the effective information of each *SC* in the signal period changes. The DSM processing effect in the quasi-periodic signal is related to the actual signal start position [3], and the optimal starting position of the actual signal needs to be determined. In theory, the larger the number of superpositions K in the DSM algorithm, the more accurate the waveform is [8], but this condition will increase computation time. Therefore, when the superimposed signal reaches the target requirement, selecting a larger K is not needed. Owing to the uncertainty of background noise, an upper limit to the noise reduction effect of the DSM method is determined, as the number of superpositions is gradually increased. When the noise reduction effect is stable, the target requirement is still not met, and the signal to be processed is considered to have failed to reduce noise.

Therefore, the adaptive noise reduction process of the synchronous hydraulic motor sound signal is the process of automatically finding the optimal superimposed length, optimal starting position, and number of times of superposition.

B. SIGNAL DENOISING METHOD BASED ON IMPROVED DSM

Based on the improved DSM, this paper proposes an adaptive noise reduction method for synchronous hydraulic motor acoustic signals. FIGURE 5 shows the flow chart of the method. The details are as follows:

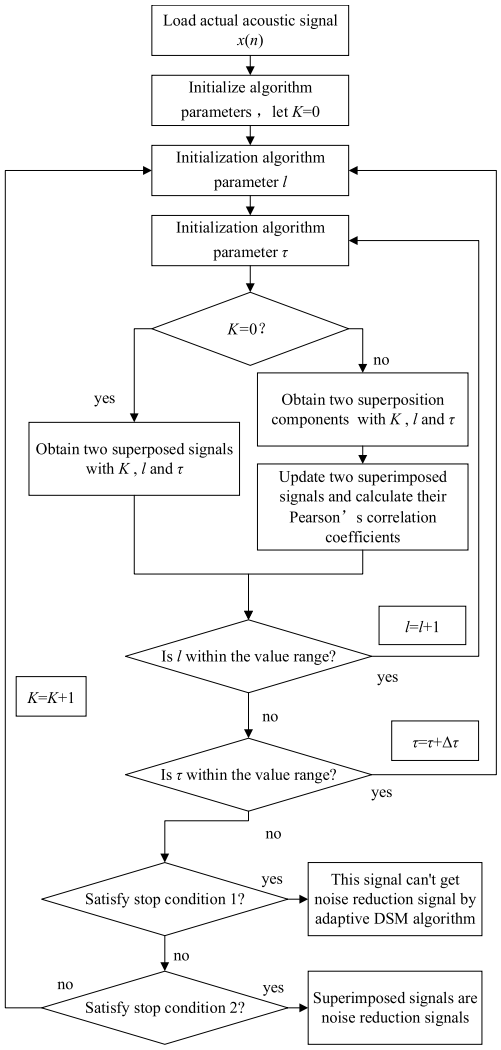

FIGURE 5. Flow chart of the acoustic signal denoising method of adaptive synchronous hydraulic motor based on improved DSM.

Step 1: Load the actual acoustic signal $x(n)$ and initialize the algorithm parameters to let $K = 0$.

Step 2: Calculate the theoretical superposition length l_0 according to the sampling frequency f_s (Hz), real-time flow velocity q (L/min), and synchronous hydraulic motor displacement V (ml/r):

$$l_0 = f_s \mathrm{V} \frac{60}{1000 \cdot q} = \frac{3\mathrm{V}f_s}{50q} \tag{5}$$

Owing to the measurement error of the flow meter, the accurate value of the measurement result is within the range of the measurement accuracy index of the flow meter; thus, l_0 may not be the optimal superimposed length. To find the optimal superimposed length, set subset of l to **F**. Set **F** to $\{(1–w)\ l_0{:}1{:}(1+w)l_0\}$, where w is the measurement accuracy of the flow meter. Finding the best starting position of the actual signal is looking for the best starting point offset τ_K^{opt}. Set τ to the actual signal start position offset, and the actual signal after the offset is recorded as $x(n+\tau)$. The subset of τ is denoted as **H**, set **H** to $\{0{:}\ l_0/a{:}\ l_0\}$.

Step 3: When $K = 0$, two superimposed signals $\tilde{x}_1(n, l, \tau)$ and $\tilde{x}_2(n, l, \tau)$ are obtained under the conditions of l and τ through the DSM algorithm. When $K \neq 0$, obtain two latest superposition components and update the superimposed signals. Compared with using equation (1) to derive the superimposed signals at the different number of superpositions, this method can improve the calculation efficiency of the algorithm. The equation of the proposed method is as follows:

$$\begin{aligned}
&\tilde{x}_1(n, l, \tau) \\
&\quad = \begin{cases} x(n+\tau), & K = 0 \\ \dfrac{1}{K+1}[K\tilde{x}_1(n, l, \tau) + x(n+2kl+\tau)], & K > 0 \end{cases} \\
&\tilde{x}_2(n, l, \tau) \\
&\quad = \begin{cases} x(n+l+\tau), & K = 0 \\ \dfrac{1}{K+1}\{K\tilde{x}_2(n, l, \tau) + x[n+(2k+1)l+\tau)]\}, & K > 0 \end{cases}
\end{aligned} \tag{6}$$

Traverse all the values of l and τ in **F**, **H**, and find the optimal superposition length l_K^{opt} and the optimal initial offset τ_K^{opt} when maximizing $\rho_{\tilde{x}_1(n,l,\tau),\tilde{x}_2(n,l,\tau)}$, and calculate the maximum correlation coefficient $\rho^{opt}(K)$ for parameters l_K^{opt} and τ_K^{opt}.

$$\begin{cases} (l_K^{opt}, \tau_K^{opt}) = \arg\max\limits_{l\in\mathbf{F},\tau\in\mathbf{Z}}[\rho_{\tilde{x}_1(n,l,\tau),\tilde{x}_2(n,l,\tau)}] \\ \rho^{opt}(K) = \rho_{\tilde{x}_1(n,l_K^{opt},\tau_K^{opt}),\tilde{x}_2(n,l_K^{opt},\tau_K^{opt})} \end{cases} \tag{7}$$

Step 4: Set two stopping conditions for the proposed algorithm. If one of the conditions is satisfied, then the procedure will not continue to search for a better noise reduction signal. When the number of superpositions is too large, and the target effect of the signal processing is still not achieved, the signal to be processed cannot be automatically reduced by the DSM method. Hence, the stop condition 1:

$$K > b \tag{8}$$

When the Pearson's correlation coefficients of the two superimposed signals meet the set requirements, the signal noise reduction is considered auspicious. Thus, stop condition 2:

$$\rho^{opt}(K) > c \tag{9}$$

If stop condition 2 is satisfied, the superimposed signals are the signals after successful noise reduction.

Step 5: When the stop conditions are not triggered, let $K = K + 1$ and recalculate from Step 2.

C. DESCRIPTION OF THE INTERNAL PARAMETERS OF THE PROPOSED METHOD

To facilitate the understanding of the proposed method, parameters a, b, and c are described below.

When the value interval of τ is too small, the calculation time is long, but when the value interval is too large, the accuracy of noise reduction waveform may be reduced. In this study, the parameter a is used to adjust the value interval of τ. When the quasi-periodic signal is relatively stable, parameter a can be taken as the larger value. When the length of each period of quasi-periodic signal changes greatly, the parameter a needs to be set as the smaller value. In this study, the operation of the synchronous hydraulic motor is stable under the test conditions. Considering the effect of the value interval, the parameter is taken as 70. When the noise reduction effect is not ideal due to the instability of the signal, we can try to increase the value of a.

Parameters b and c determine the stop condition of the algorithm, and the algorithm stops when one of the stop conditions is met.

With the increase of the number of superpositions, the improvement of noise reduction effect becomes less obvious. Therefore, parameter b is used to set the maximum the number of superpositions of the algorithm, that is, stop condition 1. According to [25], when $K = 10$, the change rate of the accuracy of the superimposed signal with K is very small, and this study sets $b = 20$ to ensure that the algorithm has enough upper limit of the number of superpositions.

In actual application, the noise reduction degree can meet the actual use requirements. Hence, parameter c is used to set the noise reduction degree of the target noise reduction signal. The larger the value of c, the more noise reduction can be expected. However, if the value of c is too large, then the specified noise reduction effect may not be achieved. This situation will increase the actual number of superpositions and then increase the noise reduction time. When $\rho^{opt}(K)$ reaches 0.6, the superposition signal $\tilde{x}_1(n, l, \tau)$ and $\tilde{x}_2(n, l, \tau)$ belong to the same signal [24]. Hence, the value range of c is set from 0.7 to 0.9 in this study.

Here are three different uses of the proposed method:

1) Let $c = 1$ and only parameter b affects the actual number of superpositions of the algorithm.

2) Let b take the larger value, and only parameter c can affect the noise reduction effect.

3) Let parameters b and c meet the actual needs, and stop the noise reduction process if any condition is met.

IV. EXPERIMENTAL CONDITIONS

FIGURE 6 is a physical diagram of a synchronous hydraulic motor test bench. The data acquisition system includes a sound sensor, data acquisition card, and a computer. The model of the sound sensor is MAX9814, which is placed beside the synchronous hydraulic motor to receive the

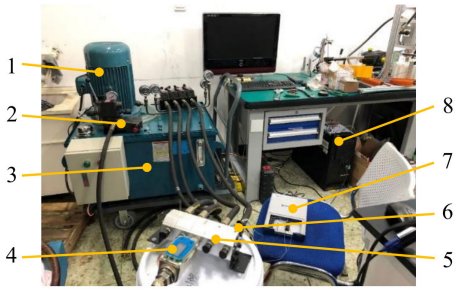

FIGURE 6. Experimental stand of the synchronous hydraulic motor. 1 Pressure gauge; 2 reversing valve and relief valve assembly; 3 fuel tank; 4 flow meter; 5 synchronous hydraulic motor; 6 acoustic sensor; 7 data acquisition card; 8 computer.

acoustic signal generated by it. The model can collect acoustic signal frequency from 20 Hz to 20 kHz. The measurement range of the flow meter is 5 to 50 L/min, and the measurement accuracy is 1%. The model of the data acquisition card is USB-6341, which was produced by National Instruments. Sampling frequency f_s is set to 20000 Hz. Data were collected and processed using MATLAB software. TABLE 1 shows the synchronous hydraulic motor models and flow parameters.

TABLE 1. Parameters of synchronous hydraulic motor.

Model	Unit	FMA-4*2.1*
Displacement	mL/r	2.17
Minimum inlet flow (750 rpm)	L/Min	6.51
Standard import flow (1500 rpm)	L/Min	13.23
Maximum import flow (3000 rpm)	L/Min	26.04
Maximum outlet pressure	MPa	21

V. EXPERIMENTAL DATA PROCESSING

FIGURE 7 is the actual acoustic signal when the synchronous hydraulic motor in the health state. At this time, the outlet pressure of the synchronous hydraulic motor is 6 MPa, and the theoretical superposition length $l_0 = 1388$ is calculated according to the flow rate $q = 7.5$ L/min. The parameters in the algorithm are set as $a = 70$, $b = 20$, and $c = 0.8$. According to the measurement accuracy of the flow meter, subset **F** is {1374:1:1402} and subset **H** is {0:20:1388}.

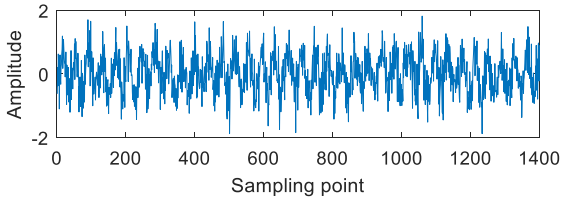

FIGURE 7. Actual acoustic signal of synchronous hydraulic motor in health state when the outlet pressure is 6 MPa.

FIGURE 8 shows the fast Fourier transform (FFT) amplitude spectrum of the actual acoustic signal of the health state of the synchronous hydraulic motor.

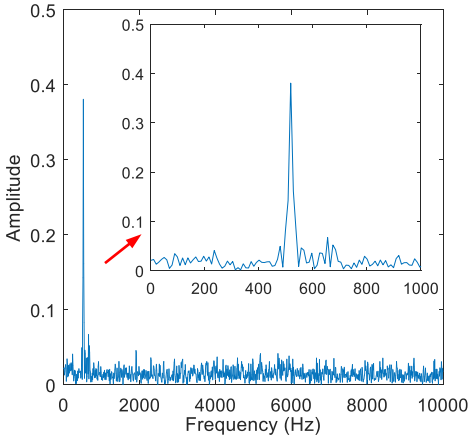

FIGURE 8. FFT amplitude spectrum of actual acoustic signal of synchronous hydraulic motor in health state.

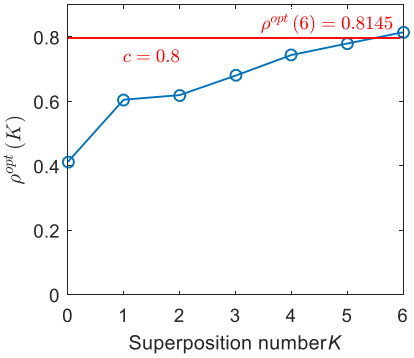

FIGURE 9. Variation curve of $\rho^{opt}(K)$ with superposition time K.

According to the calculation of real-time velocity of flow and displacement of synchronous hydraulic motor, the speed of synchronous hydraulic motor is approximately 14.4 r/s, and the tooth number of the gear is 12. Therefore, the acoustic signal with frequency of 172.8 Hz will be generated every time the gear mesh produces impact. According to the spectrum results in FIGURE 8, the frequency of the effective component of the sound signal of the health state of the synchronous hydraulic motor is approximately 510 Hz. The preliminary analysis is that each gear mesh produces three impacts. FIGURE 9 shows the change curve of $\rho^{opt}(K)$ with the superposition number K.

When $K = 6$, $\rho^{opt}(6) = 0.8145$, which satisfies stop condition 2, and the actual superposition time of adaptive noise reduction signals is 6. The actual signal is superimposed six times to obtain two noise reduction signals $\tilde{x}_1(n, l_K^{opt}, \tau_K^{opt})$ and $\tilde{x}_2(n, l_K^{opt}, \tau_K^{opt})$, and each noise reduction signal contains seven *SC*s, as shown in FIGURE 10. FIGURE 11 shows two noise reduction signals. Although the noise reduction signal still contains noise, the noise reduction effect is noticeable.

FIGURE 12 shows the FFT amplitude spectrum of the noise reduction signal of the health state of the synchronous hydraulic motor.

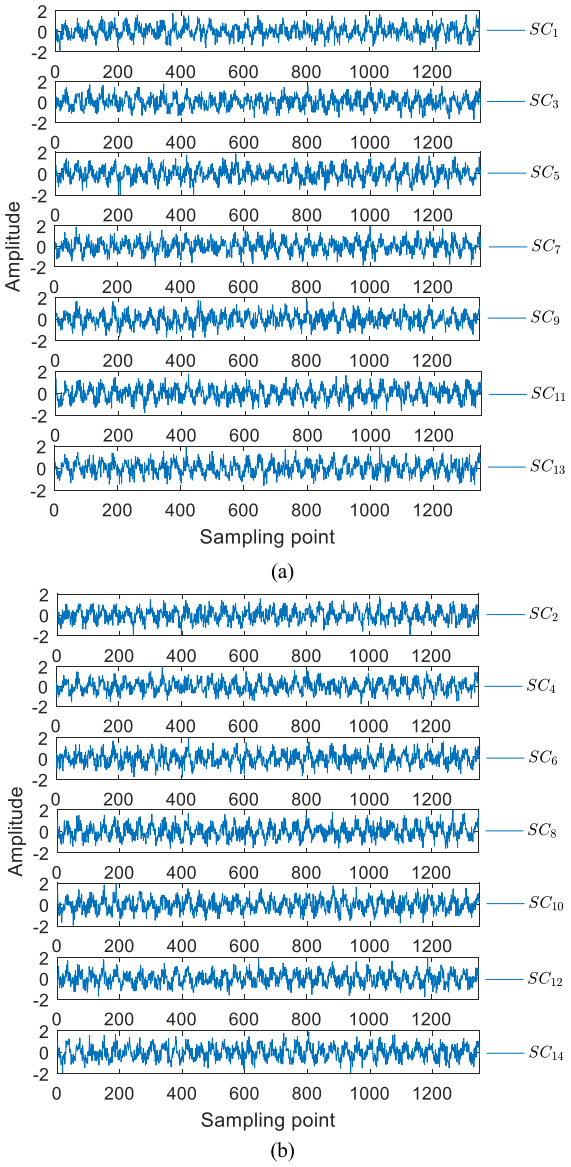

FIGURE 10. Superimposed component of the acoustic signal of the synchronous hydraulic motor is divided into two groups. (a) First group: SC_1, SC_3, SC_5, SC_7, SC_9, SC_{11}, SC_{13}. (b) Second group: SC_2, SC_4, SC_6, SC_8, SC_{10}, SC_{12}, SC_{14}.

According to spectrum results, compared with the actual sound signal, the effective component frequency of the normal noise reduction signal of the synchronous hydraulic motor has no significant change, and is still approximately 510 Hz. The spectrum amplitude of the noise component is reduced.

The results showed that the adaptive acoustic signal noise reduction method based on the improved DSM for the synchronous hydraulic motor can adaptively determine the optimal superimposed length and starting point position. Subsequently, the superimposed process runs efficiently. The entire process is simple and easy to operate without human intervention, and the processed signal has good noise reduction effect.

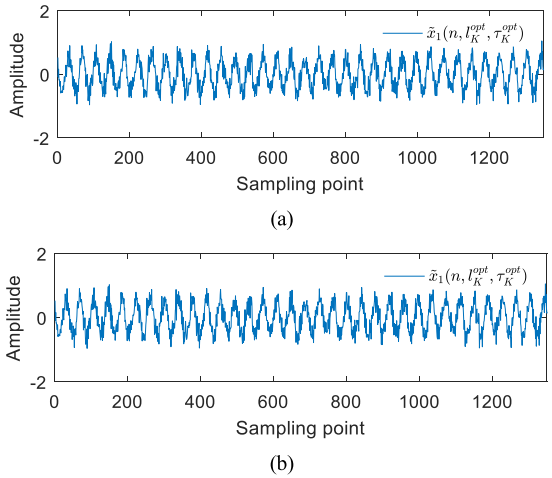

FIGURE 11. Acoustic signal of the health status of the synchronous hydraulic motor after noise reduction. (a) $\tilde{x}_1(n, l_K^{opt}, \tau_K^{opt}) = (SC_1 + SC_3 + SC_5 + SC_7 + SC_9 + SC_{11} + SC_{13})/7$. (b) $\tilde{x}_2(n, l_K^{opt}, \tau_K^{opt}) = (SC_2 + SC_4 + SC_6 + SC_8 + SC_{10} + SC_{12} + SC_{14})/7$.

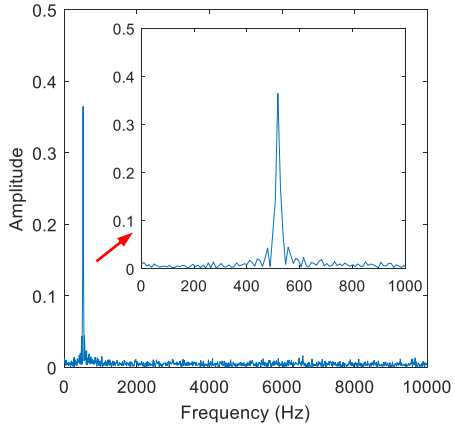

FIGURE 12. FFT amplitude spectrum of noise reduction signal of synchronous hydraulic motor in health state.

VI. OTHER APPLICATIONS OF THE PROPOSED METHOD

The acoustic signals of the synchronous hydraulic motor for the wear out state of the gear, rust state of the gear, and wear-out of the end cover of the outlet pressure of 6 MPa were collected to compare and verify the effect of the proposed method. FIGURE 13 shows the three states' physical failure parts. FIGURE 14 shows the three acoustic signal waveforms.

FIGURE 15 shows the FFT amplitude spectrum of three kinds of synchronous hydraulic motor fault signals.

According to spectrum results, three effective component frequencies of the acoustic signal of gear wears out the state of synchronous hydraulic motor, which are approximately 350 Hz, 510 Hz, and 690 Hz. The preliminary analysis indicates three different times of impact in each meshing of worn gear, which are two, three, and four times. The three are effective components in the acoustic signal of the rusty state of the gear of the synchronous hydraulic motor. The frequency is like that of the wear out state of the gear, but the

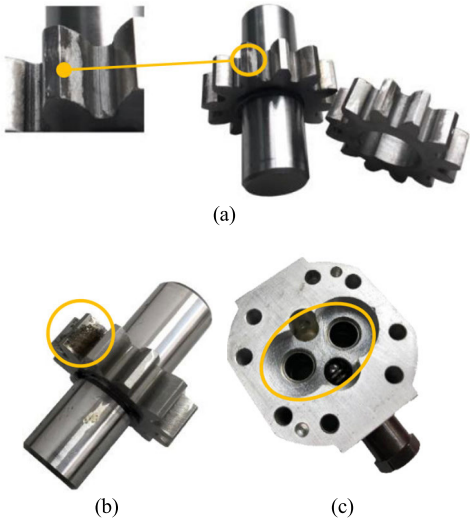

FIGURE 13. Physical failure parts. (a) Wear-out state of the gear. (b) Rust state of the gear. (c) Wear-out of the end cover.

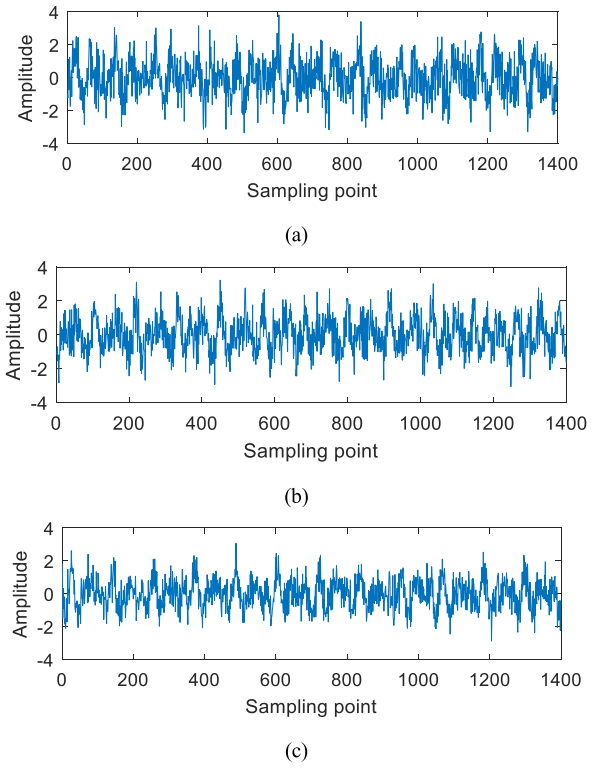

FIGURE 14. Synchronous hydraulic motor outlet pressure 6 MPa, actual acoustic signals in different states. (a) Synchronous hydraulic motor wear-out state of the gear. (b) Synchronous hydraulic motor rust state of the gear. (c) Synchronous hydraulic motor wear-out state of the end cover.

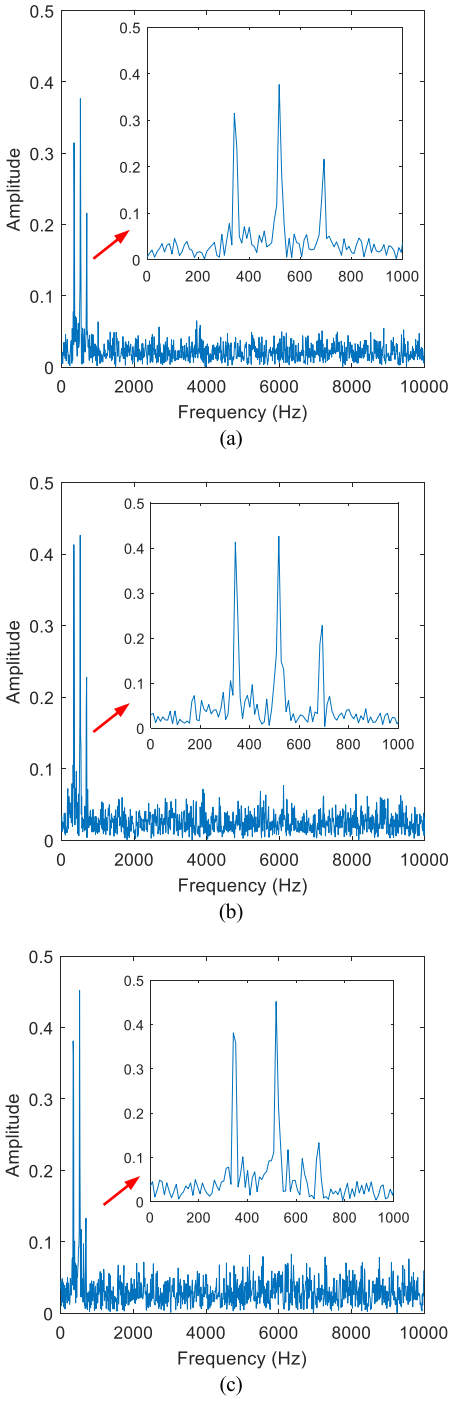

FIGURE 15. FFT amplitude spectrum of three kinds of fault acoustic signals of synchronous hydraulic motor. (a) Synchronous hydraulic motor wear-out state of the gear. (b) Synchronous hydraulic motor rust state of the gear. (c) Synchronous hydraulic motor wear-out state of the end cover.

amplitude proportion is different. The preliminary analysis shows that the contact of the rusted gear surfaces produces the acoustic signal with the same frequency as the gear wear state. The noise near the effective component frequency of the acoustic signal of the wear state of the end cover of the synchronous hydraulic motor is large, and other frequency components are mixed based on 350 Hz, 510 Hz, and 690 Hz. The preliminary analysis indicates that the wear-out part of the end cover contacts with the side of the gear to produce a variety of frequency components of the acoustic signal.

The theoretical superimposed length $l_0 = 1388$ is calculated according to the flow velocity $q = 7.5$ L/min.

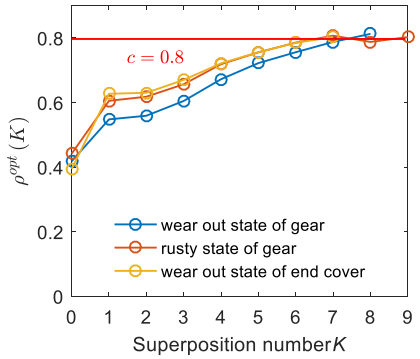

FIGURE 16. Change curve of $\rho^{opt}(K)$ in three states of the gear wear out, gear rust, and end cover wear out with the number of superpositions K. The actual superimposed times of the adaptive noise reduction signal are 8, 9, and 7.

According to the measurement accuracy of the flow meter, set subset **F** is {1318: 1: 1458} and subset **H** is {0: 20: 1388}. FIGURE 16 shows the variation curve of $\rho^{opt}(K)$ with the superposition number K.

According to FIGURE 16, $\rho^{opt}(8) < \rho^{opt}(7)$ in the result of the rust state of the gear. Preliminary analysis shows that the background noise component was superimposed and amplified to cause this phenomenon [25]. Given that superposition and amplification of background noise are accidental phenomena, the noise component can be weakened by increasing the number of superpositions. Hence, the effect on the processing effect of this method can be ignored. After the proposed adaptive noise reduction method, the noise reduction signals of three different states of the synchronous hydraulic motor are obtained, as shown in FIGURE 17.

FIGURE 18 shows FFT amplitude spectrum of noise reduction signals of three kinds of fault synchronous hydraulic motors.

According to FIGURE 18, after the noise reduction of the fault acoustic signal of the synchronous hydraulic motor by the proposed method, the amplitude of the noise frequency components in the frequency spectrum of the three states is reduced.

On the basis of the test results, the proposed method proposed has good effect on the acoustic signal processing of synchronous hydraulic motors to the wear-out state of gear, rust state of gear, and wear-out state of end cover. However, the proposed method can only deal with the situation where no drastic change happens in the mechanical speed. The reason is that the superposed length of each *SC* in the proposed method is the same. When the actual cycle length changes drastically, the optimal superimposed length cannot be found, and the superimposed process will destroy effective information in the signal. When the noise signal has the same frequency as the effective component, the superimposing process will retain both the noise and the effective component at the same time, which cannot be removed using the proposed method, the separation of signals containing multiple components requires further research.

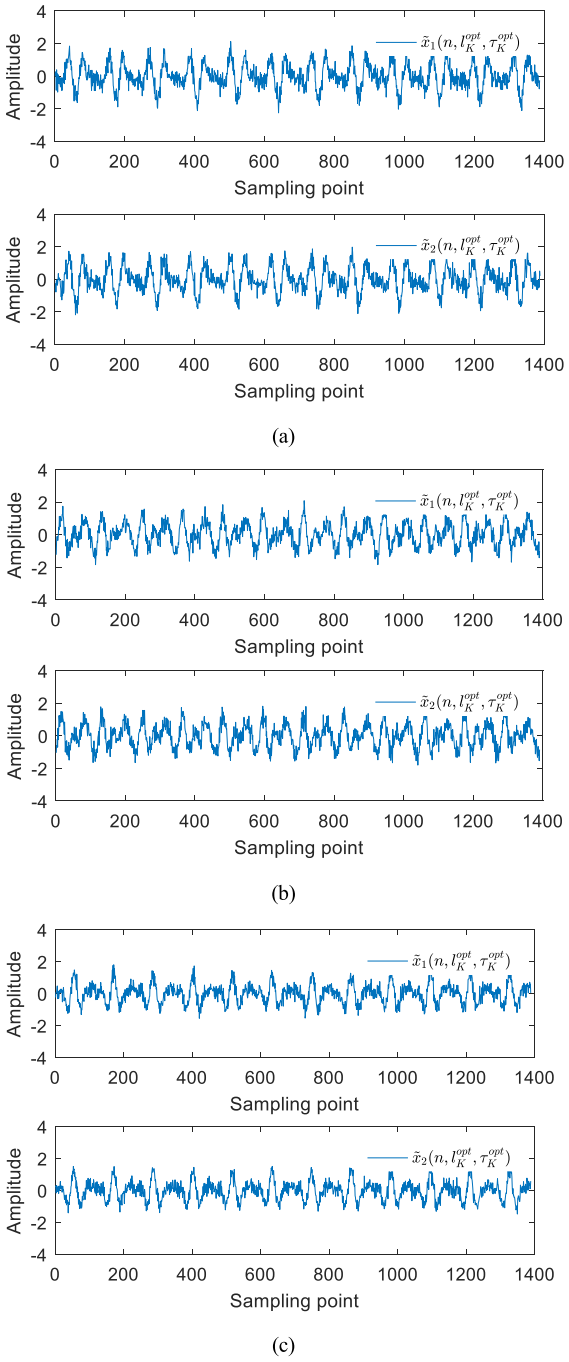

FIGURE 17. Acoustic signal of the synchronous hydraulic motor after noise reduction in different states. (a) Noise reduction signal for gear wear status. (b) Noise reduction signal for gear rust state. (c) Noise reduction signal for end cover wear-out state.

VII. COMPARATIVE ANALYSIS

To further verify the effectiveness of the proposed method, the accuracy analysis of the proposed method is performed and compared with other noise reduction methods.

A. PRECISION ANALYSIS OF THE PROPOSED METHOD

To analyze the precision of the proposed method, first, in a quiet environment, the rotating shaft of a synchronous

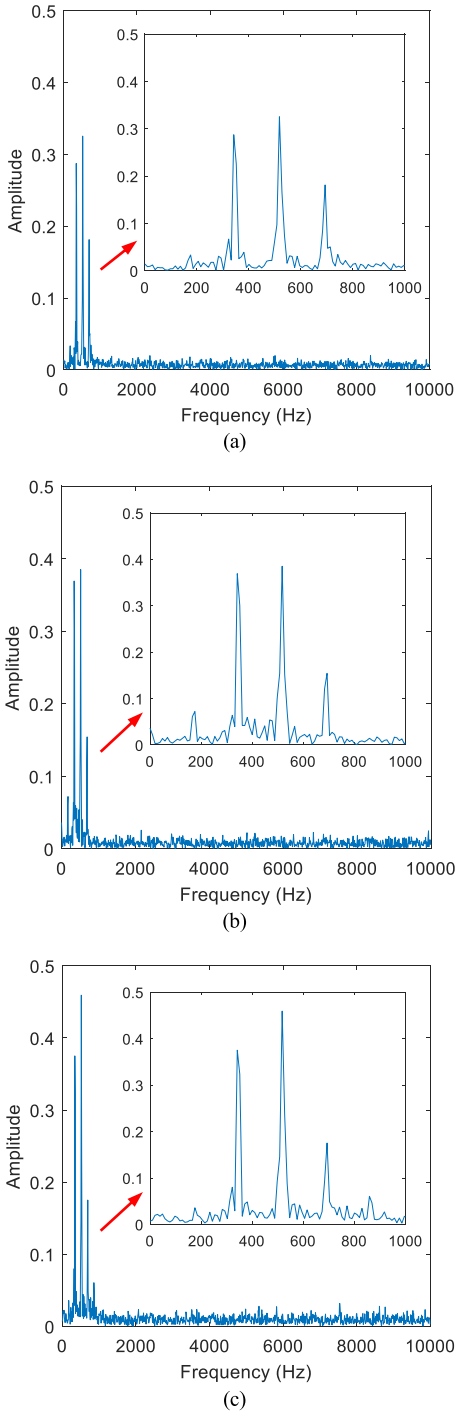

FIGURE 18. FFT amplitude spectrum of noise reduction signals of three kinds of fault synchronous hydraulic motors. (a) Noise reduction signal for gear wear status. (b) Noise reduction signal for gear rust state. (c) Noise reduction signal for end cover wear out state.

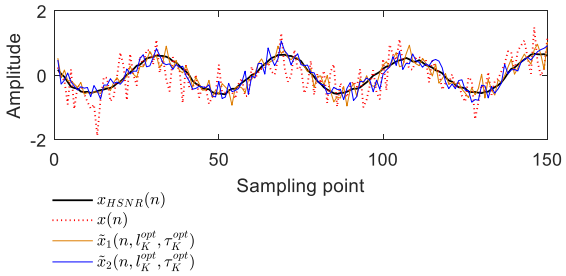

FIGURE 19. Partial waveforms of high SNR signals and actual signals and noise reduction signals of synchronous hydraulic motors in health state. $x_{HSNR}(n)$ is the high SNR ratio signal, $x(n)$ is the actual signal, $\tilde{x}_1(n, I_K^{opt}, \tau_K^{opt})$ and $\tilde{x}_2(n, I_K^{opt}, \tau_K^{opt})$ are two noise reduction signals, respective.

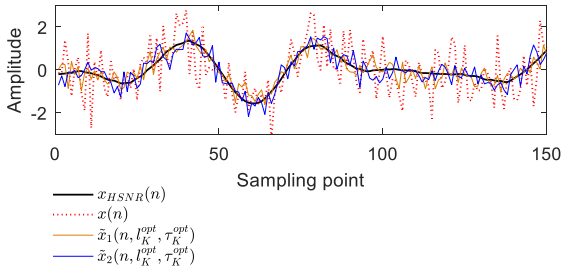

FIGURE 20. Partial waveforms of high SNR signals and actual signals and noise reduction signals of synchronous hydraulic motors in the wear out state of the gear. $x_{HSNR}(n)$ is the high SNR ratio signal, $x(n)$ is the actual signal, $\tilde{x}_1(n, I_K^{opt}, \tau_K^{opt})$ and $\tilde{x}_2(n, I_K^{opt}, \tau_K^{opt})$ are two noise reduction signals, respectively.

hydraulic motor is artificially rotated at the same speed as the above test. The acoustic signals in the four states are collected as high signal-to-noise ratio acoustic signals, which are recorded as $x_{HSNR}(n)$. The precision of the proposed method is verified by comparing the Pearson's correlation coefficients between $x_{HSNR}(n)$ with the actual signal and noise-reduced signal. The parameters in the algorithm are set to $a = 70$, $b = 20$, and $c = 0.88$. FIGURE 19 shows the local waveforms of $x_{HSNR}(n)$, $x(n)$, and the noise reduction signal of the health state's synchronous hydraulic motor. Among them, the Pearson's correlation coefficients of $x(n)$ and $x_{HSNR}(n)$ is 0.6184, and the Pearson's correlation coefficients of the noise reduction signal and $x_{HSNR}(n)$ are 0.8902 and 0.8976, respectively.

FIGURE 20 shows the local waveforms of $x_{HSNR}(n)$, $x(n)$ and the noise reduction signal of the wear out state of the synchronous hydraulic gear. Among them, the Pearson's correlation coefficient of $x(n)$ and $x_{HSNR}(n)$ is 0.6027, and the Pearson's correlation coefficients of the noise reduction signal and $x_{HSNR}(n)$ are 0.8965 and 0.9035, respectively.

FIGURE 21 shows the local waveforms of $x_{HSNR}(n)$, $x(n)$, and the noise reduction signal of the rust state of the synchronous hydraulic gear. Among them, the Pearson's correlation coefficient of $x(n)$ and $x_{HSNR}(n)$ is 0.6351, and the Pearson's correlation coefficients of the noise reduction signal and $x_{HSNR}(n)$ are 0.9033 and 0.8936, respectively.

FIGURE 22 shows the local waveforms of $x_{HSNR}(n)$, $x(n)$, and the noise reduction signal of the wear out state of the synchronous hydraulic end cover. Among them, the Pearson's correlation coefficients of $x(n)$ and $x_{HSNR}(n)$ is 0.6065, and the Pearson's correlation coefficients of the noise reduction signal and $x_{HSNR}(n)$ are 0.8988 and 0.9048, respectively.

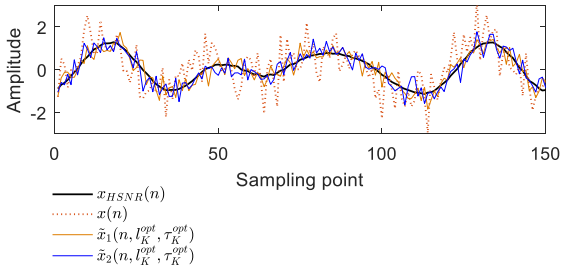

FIGURE 21. Partial waveforms of high SNR signals and actual signals and noise reduction signals of synchronous hydraulic motors in the rust state of the gear. $x_{HSNR}(n)$ is the high SNR ratio signal, $x(n)$ is the actual signal, $\tilde{x}_1(n, l_K^{opt}, \tau_K^{opt})$ and $\tilde{x}_2(n, l_K^{opt}, \tau_K^{opt})$ are two noise reduction signals, respectively.

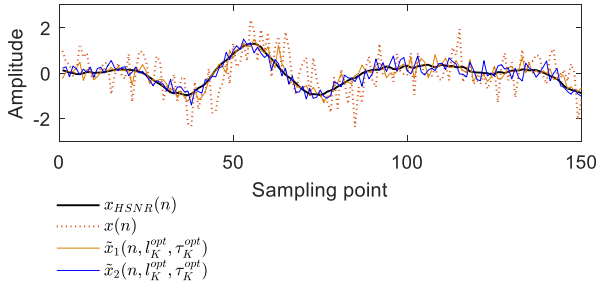

FIGURE 22. Partial waveforms of high SNR signals and actual signals and noise reduction signals of synchronous hydraulic motors in the wear out state of the end cover. $x_{HSNR}(n)$ is the high SNR ratio signal, $x(n)$ is the actual signal, $\tilde{x}_1(n, l_K^{opt}, \tau_K^{opt})$ and $\tilde{x}_2(n, l_K^{opt}, \tau_K^{opt})$ are two noise reduction signals, respectively.

According to the analysis results, compared with the actual signal, the noise reduction signal of the synchronous hydraulic motor obtained by the proposed method is closer to the high SNR waveform. When the received noise reduction signal is not ideal, the noise reduction effect can be enhanced by adjusting the values of parameters a, b, and c.

B. COMPARISON WITH OTHER NOISE REDUCTION METHODS

To analyze fully the noise reduction effect and time efficiency of the proposed algorithm, the time-domain synchronous averaging method, soft threshold wavelet denoising, and S-G filter were used to reduce the noise of the synchronous hydraulic motor acoustic signal and compared with the proposed method. The number of superimpositions of the proposed method and the time-domain synchronous averaging method are set to 10. The wavelet base in soft threshold wavelet denoising is set to db4, the number of decomposition layers to 5, and the remaining parameters to default values. The S-G filter's polynomial order is set to 3 and the frame length is set to 11. The Pearson's correlation coefficients of their noise reduction and high signal-to-noise ratio signals are calculated. TABLE 2 shows the noise reduction processing accuracy effects of the four methods on the four states of the synchronous hydraulic motor. The proposed method is expressed as ''improved DSM.''

TABLE 2. Noise reduction precision results of acoustic signal of synchronous hydraulic motor.

Type	Improved DSM	Time-domain synchronous averaging	Soft threshold wavelet denoising	S-G filter
Health state	0.9306	0.6216	0.8031	0.8101
Wear-out state of the gear	0.9227	0.5834	0.8256	0.7924
Rust state of the gear	0.9215	0.4394	0.8721	0.6902
Wear-out state of the end cover	0.9177	0.6425	0.8231	0.8131

TABLE 3. Time-averaged calculation results of the noise reduction process of the synchronous hydraulic motor acoustic signals from three methods.

Type	Improved DSM	Time-domain synchronous averaging	Soft threshold wavelet denoising	S-G filter
Time(s)	6.1887	0.0561	0.0427	0.0131

According to the results, the proposed method has higher noise reduction accuracy for the acoustic signals of synchronous hydraulic motors than soft threshold wavelet denoising, time-domain synchronous averaging, and S-G filter. To compare further the noise reduction process of the three methods, the average calculation time of the acoustic signal of the synchronous hydraulic motor is calculated for each method. The average calculation time of each method, which is defined as the average value of the noise reduction time of the four states of the synchronous hydraulic motor, is calculated. Four kinds of noise reduction methods are implemented in the MATLAB software on the PC side. The CPU model of the PC is i5-7400, the RAM size is 8 G, and the hard disk type is HHD. TABLE 3 shows the results of the average calculation time of the noise reduction process of the synchronous hydraulic motor acoustic signals by the three methods.

According to the results, the calculation time of the improved DSM is longer than that of the time-domain synchronous averaging method, wavelet noise reduction method, and S-G filter. This result was due to the large data requirement of the improvement of DSM to perform cyclic calculations to find the optimal starting position and the optimal superimposed length. Such step results in longer time taken by this method.

Therefore, when comprehensively comparing noise reduction accuracy and reduction, the proposed method is more suitable for occasions where the degree of real-time noise reduction is not high.

VIII. CONCLUSION

Traditional DSM can only artificially find the superimposed length and start position of the quasi-periodic signal but cannot automatically process the quasi-periodic acoustic signal of a synchronous hydraulic motor. On the basis of the improved DSM, this study proposes an adaptive noise reduction method for the acoustic signal of a synchronous hydraulic motor. This method realizes the automatic noise reduction of four acoustic signals of the synchronous hydraulic motor health states, namely, gear wear-out state, gear rust state, and end cover wear-out state. The proposed method can automatically obtain the optimal superimposed length of the quasi-periodic signal, signal starting position, and superposition number. This method is simple and easy to achieve, and the degree of noise reduction can be adjusted through parameters, and the noise reduction effect is significant. Moreover, the method improves the applicability of the misalignment superposition algorithm and adds noise reduction processing on the time domain signal. The proposed method has higher noise reduction accuracy than the time-domain synchronous averaging method and wavelet noise reduction when processing the acoustic signals of synchronous hydraulic motors, but the noise reduction process takes too long. Hence, the calculation efficiency can be used as a research method to continue in-depth research. The proposed method can be used for automatic noise reduction of quasi-periodic signals of other rotating machinery.

ACKNOWLEDGMENT

The authors would like to thank the editor and peer reviewers for their efforts.

REFERENCES

[1] A. Glowacz, "Recognition of acoustic signals of commutator motors," *Appl. Sci.*, vol. 8, no. 12, p. 2630, Dec. 2018.
[2] A. Glowacz, "Fault detection of electric impact drills and coffee grinders using acoustic signals," *Sensors*, vol. 19, no. 2, p. 269, Jan. 2019.
[3] N. Dayong, J. Yuhua, S. Hongyu, Z. Zengmeng, G. Yongjun, C. Shengtao, and H. Jiaoyi, "Separation method of impulsive fault component for gasoline engine based on acoustic signal analysis," *Shock Vib.*, vol. 2019, pp. 1–15, Apr. 2019, doi: 10.1155/2019/8573479.
[4] I. S. Bozchalooi and M. Liang, "A joint resonance frequency estimation and in-band noise reduction method for enhancing the detectability of bearing fault signals," *Mech. Syst. Signal Process.*, vol. 22, no. 4, pp. 915–933, May 2008.
[5] M. Srivastava, C. L. Anderson, and J. H. Freed, "A new wavelet denoising method for selecting decomposition levels and noise thresholds," *IEEE Access*, vol. 4, pp. 3862–3877, 2016.
[6] N. E. Huang, Z. Shen, S. R. Long, M. C. Wu, H. H. Shih, Q. Zheng, N.-C. Yen, C. C. Tung, and H. H. Liu, "The empirical mode decomposition and the Hilbert spectrum for nonlinear and non-stationary time series analysis," *Proc. Roy. Soc. London. A, Math., Phys. Eng. Sci.*, vol. 454, no. 1971, pp. 903–995, Mar. 1998.
[7] J. Chen, T. Jin, M. A. Mohamed, and M. Wang, "An adaptive TLS-ESPRIT algorithm based on an S-G filter for analysis of low frequency oscillation in wide area measurement systems," *IEEE Access*, vol. 7, pp. 47644–47654, 2019.
[8] N. Dayong, S. Changle, G. Yongjun, Z. Zengmeng, and H. Jiaoyi, "Extraction of fault component from abnormal sound in diesel engines using acoustic signals," *Mech. Syst. Signal Process.*, vol. 75, pp. 544–555, Jun. 2016.
[9] J. Cai, "Gear fault diagnosis based on a new wavelet adaptive threshold de-noising method," *Ind. Lubrication Tribol.*, vol. 71, no. 1, pp. 40–47, Jan. 2019.
[10] A. Parey and A. Singh, "Gearbox fault diagnosis using acoustic signals, continuous wavelet transform and adaptive neuro-fuzzy inference system," *Appl. Acoust.*, vol. 147, pp. 133–140, Apr. 2019.
[11] J. Wang and Q. He, "Wavelet packet envelope manifold for fault diagnosis of rolling element bearings," *IEEE Trans. Instrum. Meas.*, vol. 65, no. 11, pp. 2515–2526, Nov. 2016.
[12] S. N. Chegini, A. Bagheri, and F. Najafi, "Application of a new EWT-based denoising technique in bearing fault diagnosis," *Measurement*, vol. 144, pp. 275–297, Oct. 2019.
[13] J. Chen, X. Li, M. A. Mohamed, and T. Jin, "An adaptive matrix pencil algorithm based-wavelet soft-threshold denoising for analysis of low frequency oscillation in power systems," *IEEE Access*, vol. 8, pp. 7244–7255, 2020.
[14] Wang and Lee, "Fault diagnosis of a helical gearbox based on an adaptive empirical wavelet transform in combination with a spectral subtraction method," *Appl. Sci.*, vol. 9, no. 8, p. 1696, Apr. 2019, doi: 10.3390/app9081696.
[15] Y. Qin, J. Wang, and Y. Mao, "Dense framelets with two generators and their application in mechanical fault diagnosis," *Mech. Syst. Signal Process.*, vol. 40, no. 2, pp. 483–498, Nov. 2013.
[16] Y. Qin, Y. Mao, B. Tang, Y. Wang, and H. Chen, "M-band flexible wavelet transform and its application to the fault diagnosis of planetary gear transmission systems," *Mech. Syst. Signal Process.*, vol. 134, Dec. 2019, Art. no. 106298.
[17] J. Zheng, H. Pan, S. Yang, and J. Cheng, "Adaptive parameterless empirical wavelet transform based time-frequency analysis method and its application to rotor rubbing fault diagnosis," *Signal Process.*, vol. 130, pp. 305–314, Jan. 2017.
[18] H. Li, B. Yu, B. Qing, and S. Luo, "Cavitation pulse extraction and centrifugal pump analysis," *J. Mech. Sci. Technol.*, vol. 31, no. 3, pp. 1181–1188, Mar. 2017.
[19] Z. Zhang, X. Liu, R. Shu, F. Xie, F. Wang, Z. Liu, H. Zhang, and Z. Wang, "A novel noise reduction method for space-borne full waveforms based on empirical mode decomposition," *Optik*, vol. 202, Feb. 2020, Art. no. 163581, doi: 10.1016/j.ijleo.2019.163581.
[20] G. Li, Q. Guan, and H. Yang, "Noise reduction method of underwater acoustic signals based on CEEMDAN, effort-to-compress complexity, refined composite multiscale dispersion entropy and wavelet threshold denoising," *Entropy*, vol. 21, no. 1, p. 11, Dec. 2018, doi: 10.3390/e21010011.
[21] G. Li, Z. Yang, and H. Yang, "Noise reduction method of underwater acoustic signals based on uniform phase empirical mode decomposition, amplitude-aware permutation entropy, and pearson correlation coefficient," *Entropy*, vol. 20, no. 12, p. 918, Nov. 2018, doi: 10.3390/e20120918.
[22] S. Liu, Y. Sun, W. Ma, F. Xie, X. Jiang, L. He, and Y. Kang, "A new signal processing method based on notch filtering and wavelet denoising in wire rope inspection," *J. Nondestruct. Eval.*, vol. 38, no. 2, Mar. 2019.
[23] Q. Li and S. Y. Liang, "Weak crack detection for gearbox using sparse denoising and decomposition method," *IEEE Sensors J.*, vol. 19, no. 6, pp. 2243–2253, Mar. 2019.
[24] S. M. Stigler, "Francis Galton's account of the invention of correlation," *Stat. Sci.*, vol. 4, no. 2, pp. 73–79, May 1989.
[25] J. Benesty, J. Chen, and Y. Huang, "On the importance of the pearson correlation coefficient in noise reduction," *IEEE Trans. Audio, Speech, Lang. Process.*, vol. 16, no. 4, pp. 757–765, May 2008.